



High resolution modelling of wind fields for optimization of empirical storm flood predictions

B. Brecht and H. Frank

Deutscher Wetterdienst, Offenbach, Germany

Correspondence to: B. Brecht (benedict-manuel.brecht@dwd.de)

Received: 15 January 2014 – Revised: 19 March 2014 – Accepted: 20 March 2014 – Published: 6 May 2014

Abstract. High resolution wind fields are necessary to predict the occurrence of storm flood events and their magnitude. Deutscher Wetterdienst (DWD) created a catalogue of detailed wind fields of 39 historical storms at the German North Sea coast from the years 1962 to 2011. The catalogue is used by the Niedersächsisches Landesamt für Wasser-, Küsten- und Naturschutz (NLWKN) coastal research center to improve their flood alert service.

The computation of wind fields and other meteorological parameters is based on the model chain of the DWD going from the global model GME via the limited-area model COSMO with 7 km mesh size down to a COSMO model with 2.2 km. To obtain an improved analysis COSMO runs are nudged against observations for the historical storms. The global model GME is initialised from the ERA reanalysis data of the European Centre for Medium-Range Weather Forecasts (ECMWF).

As expected, we got better congruency with observations of the model for the nudging runs than the normal forecast runs for most storms. We also found during the verification process that different land use data sets could influence the results considerably.

1 Introduction

Storm floods at coastal regions are natural phenomena occurring at irregular intervals and variable intensity. The three biggest storm floods at the German North Sea coast in the 20th century occurred in the years 1962, 1976 and 1999. The flood in 1976 reached the highest water levels at almost all German North Sea stations. Nevertheless the flood of Hamburg in 1962 caused much more damage and 315 fatal casualties (Jensen et al., 2006). In the 21st century three very severe storm floods, with a water level of at least 3.5 m over the mean high water level (MHW), occurred in the years 2006, 2007 and 2013 (e.g. Wiegand, 1990; BSH, 2014).

The central target of the project “OptempS-MohoWif” (High resolution modelling of wind fields for optimization of empirical storm flood predictions) is an improvement of the regional storm flood alert service at the North Sea coast of Lower Saxony. The project is divided into two parts. The first part of the project concerning the wind fields is done by Deutscher Wetterdienst (DWD). The second part con-

cerning water level modeling is done by the flood alert service of Niedersächsisches Landesamt für Wasser-, Küsten- und Naturschutz (NLWKN). To improve their flood model, highly-resolved spatial and temporal wind fields of severe storms are necessary, which are provided by the DWD.

Therefore, a catalogue of 39 historical storms, which lead to storm floods at the German North Sea coast from the years 1962 to 2011, was created (see Table 1). Each storm event was simulated for about 4–5 days, except for two events with 7 and 11 days respectively, when several storms are connected. The forecast of an event starts three days before the highest water level occurs. It ends one or two low tides after the maximum water level. The simulations of the meteorological fields are computed by the model chain of DWD, which is started from reanalysis data of ECMWF (European Centre for Medium-Range Weather Forecasts). To verify the simulations the meteorological fields are compared with observational data of up to 25 stations at the German, Dutch and Danish North Sea coast, or stations in the North Sea like platforms or fire ships.

In 2005 there was a similar project for 22 storms from 1962 until 2002 (Frank and Majewski, 2006). The major improvements in the new project are the nudging of the COSMO simulations to observations as well as newer model versions, higher resolution, greater model domain, and more frequent reanalysis data used by GME.

In the following section the model setup and the nudging process are described. Then the verification procedure is shown, in presenting the results of one selected storm, followed by the demonstration of the results for the set of the storms. Finally, the most important information are summarized.

2 Model chain

The model chain of the DWD consists of the global model GME (Majewski et al., 2002) and the limited-area non-hydrostatic model COSMO (COSMO model documentation, 2014), which is run in the two versions COSMO-eu and COSMO-de. GME is a hydrostatic model operating on an icosahedral grid. For these simulations a mesh width of 30 km and 60 vertical layers is used whereas, operationally, GME runs on a 20 km grid. Here, GME is initialized four times a day (00:00, 06:00, 12:00, and 18:00 UTC) from reanalysis data of ECMWF. For storms in and after 1979 the ERAInterim reanalysis data (Dee et al., 2011) is used. Before 1979 we use ERA-40 reanalysis data (Uppala et al., 2005). GME provides initial and boundary data for COSMO-eu with a mesh width of 7 km and 40 vertical layers. COSMO-eu in turn drives COSMO-de which has a mesh width of 2.2 km and 65 vertical layers. At this resolution deep convection can be explicitly resolved (Baldauf et al., 2011). Therefore, only shallow convection is parametrized in COSMO-de. Compared to the operational COSMO-EU at the DWD, the domain of COSMO-eu is decreased in the south and the east (see Fig. 1), as these regions are not important for storm flood predictions at the North Sea coast. COSMO-de is increased in the north, west and south compared to the operational COSMO-DE (see Fig. 1). The vertical resolution is increased from operationally 50 to 65 layers. COSMO-de serves as test bed for a possible new operational setup of COSMO-DE.

In a first series of experiments the model chain was started by a new reanalysis field every 6 h and run to 18 h. 6-hourly segments of the 18 h forecasts were connected to get a continuous time series with minimal jumps from one forecast to the next. Tests were run, in order to determine which segments yielded the minimal root mean square difference of mean sea level pressure (p.m.s.l.) from the end of a segment to the start of the segments of the next forecast, for example “p.m.s.l.(00:00 UTC + 8 h)–p.m.s.l.(06:00 UTC + 2 h)”. This test was made for 3 complete storms. It was found that the RMSE at “X UTC + 10 h–(X+6) UTC + 4 h” was minimal. Therefore the hours 5–10 of every 18 h forecast are used and connected to a continuous time series to obtain the forecast

Domains COSMO–EU and COSMO–DE

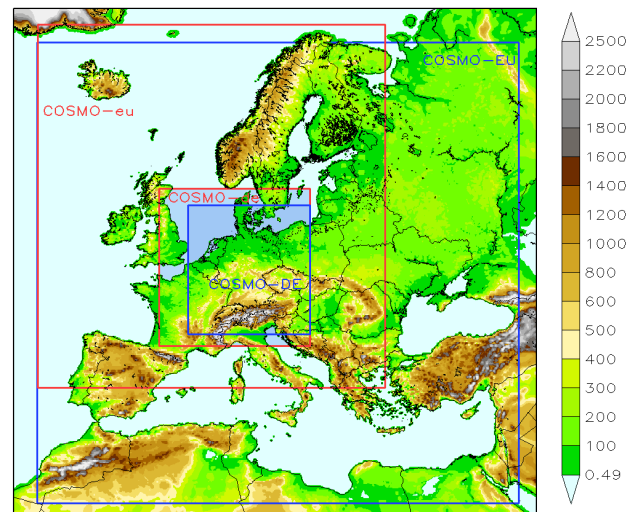


Figure 1. Domains of COSMO: the red lines show the domains of the 7 km COSMO-eu, and 2.2 km COSMO-de. The blue lines show the domains of the operational versions COSMO-EU and COSMO-DE.

with the minimal jump of p.m.s.l. between two consecutive forecasts of one storm.

2.1 Nudging runs

In order to get an improved analysis at high resolution, the simulations with COSMO have additionally been carried out with the Newtonian relaxation or nudging technique (Stauffer et al., 1990) to obtain one continuous analysis without jumps. With this method the prognostic variables of the model are relaxed towards prescribed values within a period of time (Schraff, 1997). In this case the prescribed values are direct observations, which is advantageous for synoptic observations (Stauffer and Seaman, 1994). The relaxation against the observations is done via additional terms in the prognostic equations. In practical applications, the nudging term should and usually does remain smaller than the largest term of the dynamics. This situation is related to the basic idea of the method that the model fields are to be relaxed towards the observed values without significantly disturbing the dynamic balance of the model (Schraff and Hess, 2002).

Observations are used from radiosondes (horizontal wind, temperature, humidity and pressure), aircraft measurements (horizontal wind and temperature), wind profiler (horizontal wind) and surface observations (10 m wind, only used for stations below 100 m above sea level to select only stations in flat terrain).

The observations are obtained from the DWD archives, which date back until 1966. Hence, for the first storm in 1962 no nudging run is available. For the nudging runs the

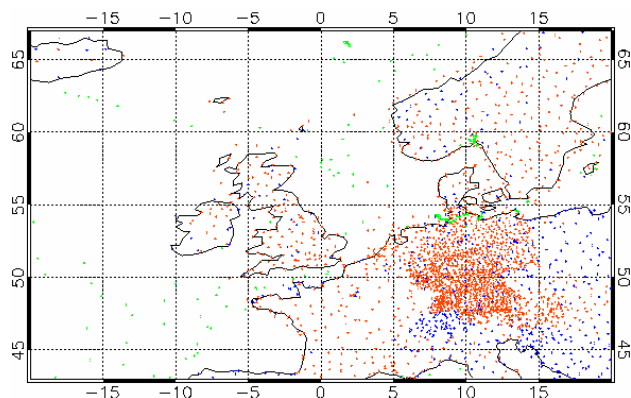


Figure 2. Data coverage of Synop land and ship observations on 9 November 2007. The blue dots show the manned land stations, the red dots the automatic land stations and the green dots the ships.

observations are processed with the same quality control procedure as the operational runs.

A more detailed description of the nudging in COSMO is given by Schraff and Hess (2002).

The nudging runs of COSMO were made in segments of 6 h. However, a new segment is started from the last analysis of the previous segment. Hence, each storm analysis is simulated in a continuous analysis cycle, which is initialized from the reanalysis data only at the very start of the storm event.

2.1.1 Availability of Nudging data

The data availability increases from older to more recent storms. The total available observations per 6 h for the COSMO-eu area are 2000–3000 Synop land and ship (relation 10 : 1) observations for events from 1966–1976. In 1977 it increased to approximately 5000 per 6 h mainly due to an increased frequency of Synop measurements (to 3 hourly or hourly observations), and due to the first use of drifting buoys and aircraft observations. Until the year 2000 it slowly increased up to 15 000 observations per year. Radiosonde data have been available since 1991, and wind profiler data have been available since 2000. Since 2006 over 40 000 observations in 6 h are available. As an example, Fig. 2 shows the coverage of available Synop land and ship observations on 9 November 2007 during storm “Tilo”.

The used data are less than the available data caused by the quality control, the availability of meta information like station height, or differences between real station height and model orography. Approximately 40 % to 90 % of the available data are used for the nudging.

For the storms from 1966–1976 only 40–50 % of the data are used by the model, mostly due to missing station altitudes of Synop land stations. From 1977–2000 80–90 % of the measurements are accepted. For later runs this ratio decreases again to 60–65 %.

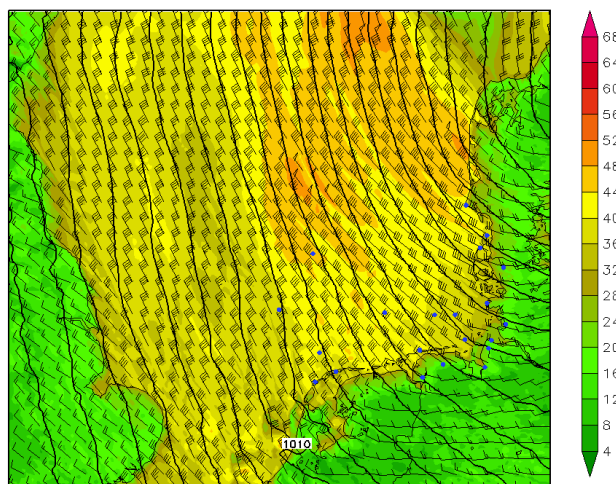


Figure 3. Wind field over the North Sea of storm “Tilo” at 9 November 2007, 06:00 UTC, 3 h before the water reached the highest level at Norderney. Shown is a COSMO-de nudging run. The wind 10 m above ground is shown in knots. As contour lines p.m.s.l. is shown in 2 hPa intervals. The blue dots show the locations of the stations which were used for verification.

3 Results

The COSMO model data were verified with observations of up to 25 Synop stations at or near the North Sea coast of Denmark, Germany and the Netherlands, as well as some stations in the North Sea (platforms, fire ships). Except for one station (Scharhörn, external data), these stations were also used in the nudging runs we made. However, not all stations were available for all storms. The verification was made for sea level pressure, p.m.s.l., wind speed at 10 m, v_{10m} , and wind direction at 10 m, dd_{10m} . We calculated the bias of the model (model-obs), and the RMSE of the model values vs. the observation values. In the next section we present results for storm “Tilo” in 2007, accordingly we present the general results for all 39 simulated storms.

3.1 Verification of storm “Tilo” 2007

Storm “Tilo” passed from the south of Iceland to the west coast of Norway and to the North of the Skagerrak. For many hours the water was pushed by northwesterly winds into the German Bight, see Fig. 3, which resulted in the high water level. As is typical for Northern Hemisphere mid-latitude storms the strongest winds of “Tilo” occurred on the southwest side of the low pressure centre behind the cold front.

For the verification of storm “Tilo” we verified data of 21 stations. We can compare both COSMO models as well as nudging runs with forecast runs (see Fig. 4). For COSMO-eu the RMSE and biases for all 3 variables, v_{10m} , dd_{10m} , and p.m.s.l., are less for the nudging analysis than for the forecast runs. The biases are $1.1 \pm 1.1 \text{ m s}^{-1}$ compared to

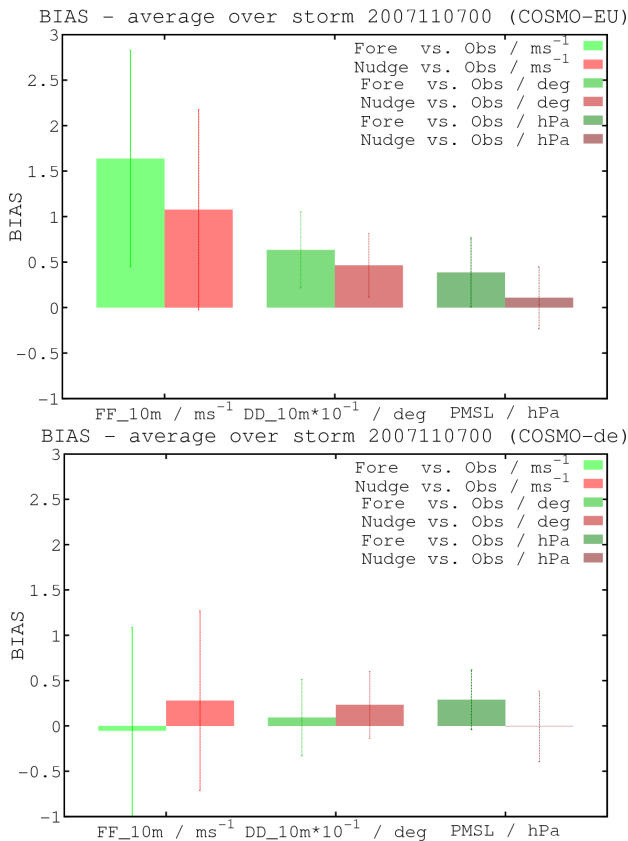


Figure 4. The biases and uncertainties of the biases for storm “Tilo” for the three variables v_{10m} , dd_{10m} and p.m.s.l. for COSMO-eu and COSMO-de and both for nudging runs (red) and runs without nudging (green). At the top the biases for COSMO-eu and at the bottom the biases for COSMO-de are shown.

$1.6 \pm 1.2 \text{ m s}^{-1}$, $4.6 \pm 3.4^\circ$ vs. $6.3 \pm 4.2^\circ$, and $0.1 \pm 0.3 \text{ hPa}$ vs. $0.4 \pm 0.3 \text{ hPa}$ (see Fig. 4, top). The uncertainties of the values presented here are the standard deviations over all observation stations.

The RMSE values are $2.2 \pm 0.6 \text{ m s}^{-1}$ vs. $2.7 \pm 0.8 \text{ m s}^{-1}$, $13.0 \pm 4.2^\circ$ vs. $15.6 \pm 4.5^\circ$, and $0.5 \pm 0.2 \text{ hPa}$ vs. $0.8 \pm 0.2 \text{ hPa}$. For this storm, the results of the nudging run were better than for the forecast run for all variables. The results for the biases also show that the variances of the observations are not negligible. The variances for v_{10m} and dd_{10m} can arise from the difference of land and sea observations and if their nearest grid points of the model are land or sea points.

COSMO-de showed qualitatively similar behaviour for the RMSE, but differences in the bias. The RMSE of the nudging runs versus the normal forecast runs were $2.0 \pm 0.5 \text{ m s}^{-1}$ vs. $2.2 \pm 0.6 \text{ m s}^{-1}$, $13.4 \pm 5.0^\circ$ vs. $14.5 \pm 4.3^\circ$, and $0.5 \pm 0.2 \text{ hPa}$ vs. $0.8 \pm 0.2 \text{ hPa}$ for p.m.s.l. Hence, the nudging run was slightly better than the run without nudging. But, the bias showed no unambiguous tendency between the two modes (see Fig. 4, bottom).

Table 1. Catalogue of the 39 historical storm floods and the RMSE and bias of the wind speed (v_{10} , m s^{-1}) for COSMO-eu (eu) and COSMO-de (de) forecast runs (fo) and nudging runs (an). The first three columns show the storm number (No), the start date (UTC) and the duration (Dur) of a storm (in days, d). An event lasts from approximately 3 days before the main maximum water level until one or two low tides later. Simulations start at 00:00 UTC of the first day and end at 24:00 UTC of the last day.

No	Start	Dur	RMSE		bias	
			eu v_{10} an/fo	eu v_{10} an/fo	de v_{10} an/fo	de v_{10} an/fo
1	1962-02-14	4 d	–	–	–	–
2	1966-11-28	4 d	2.9/2.6	0.5/0.7	2.9/2.6	–0.1/–0.1
3	1967-02-21	4 d	3.0/3.4	–0.3/–0.3	3.6/3.9	–0.5/–0.8
4	1967-02-26	4 d	2.2/2.5	0.2/0.2	2.3/2.6	–0.5/–0.4
5	1973-11-10	11 d	3.4/3.4	0.7/1.0	3.9/3.7	0.6/0.1
6	1973-12-04	4 d	2.6/2.8	0.7/1.4	3.1/3.1	0.7/0.8
7	1973-12-11	4 d	3.0/2.8	1.3/1.4	3.2/3.2	1.0/1.0
8	1976-01-01	4 d	3.4/3.2	–0.2/1.0	3.8/3.3	–0.7/0.1
9	1976-01-18	5 d	2.7/2.6	0.1/0.9	3.5/3.3	–0.6/–0.3
10	1977-12-28	4 d	2.4/2.9	0.1/1.0	2.8/3.3	–0.4/0.1
11	1981-11-21	5 d	2.4/2.6	0.1/1.0	2.8/3.0	–0.6/–0.2
12	1983-01-30	4 d	3.2/3.2	–0.1/0.4	2.1/2.3	–0.8/–0.6
13	1988-12-02	4 d	1.8/2.0	0.6/0.9	1.8/1.7	0.0/0.0
14	1989-02-11	5 d	2.1/2.2	0.3/0.6	2.2/2.3	–0.7/–0.5
15	1990-01-23	5 d	2.4/2.4	0.6/0.7	2.8/2.6	–0.7/–0.8
16	1990-02-24	5 d	2.2/2.5	0.0/0.1	2.6/2.8	–1.0/–1.1
17	1990-08-18	4 d	1.6/2.0	0.0/0.0	1.9/2.2	–0.2/–0.9
18	1991-12-17	5 d	1.9/2.2	0.1/0.3	2.1/2.2	–0.4/–0.5
19	1993-01-20	4 d	2.0/2.2	0.1/0.1	2.9/2.8	–1.5/–1.6
20	1993-12-07	4 d	2.0/2.3	0.0/0.4	2.3/2.4	–0.5/–0.7
21	1993-12-17	4 d	1.8/1.9	0.0/0.3	2.2/2.3	–0.7/–0.9
22	1994-01-25	7 d	2.1/2.2	–0.4/–0.1	2.4/2.5	–0.9/–1.0
23	1994-03-11	4 d	1.7/1.8	–0.3/0.3	2.3/2.2	–1.0/–0.9
24	1994-12-30	4 d	2.3/2.6	0.1/0.6	2.5/2.7	–0.3/–0.6
25	1995-01-07	5 d	1.8/2.4	0.4/1.0	1.9/2.2	0.1/0.3
26	1996-10-27	4 d	1.9/2.3	0.4/1.1	2.0/2.1	–0.2/–0.2
27	1999-02-02	5 d	1.9/2.0	0.2/0.3	2.0/2.1	–0.4/–0.7
28	1999-11-30	5 d	2.4/2.5	0.9/1.1	2.4/2.4	–0.1/–0.6
29	2000-01-27	4 d	1.8/1.9	0.5/0.8	2.0/2.0	–0.5/–0.3
30	2002-10-25	4 d	2.2/2.4	0.4/0.7	2.2/2.4	–0.2/–0.4
31	2006-10-29	4 d	2.1/2.3	0.9/1.2	1.9/2.0	–0.1/–0.3
32	2007-01-09	4 d	2.4/2.8	1.0/1.5	2.2/2.3	–0.6/–0.5
33	2007-01-16	4 d	2.2/2.5	1.1/1.4	2.0/2.3	0.0/0.0
34	2007-03-16	5 d	2.0/2.2	0.4/0.6	1.9/2.1	0.2/0.4
35	2007-11-07	4 d	2.2/2.7	1.1/1.6	2.0/2.2	0.3/–0.1
36	2007-11-23	4 d	2.0/2.4	0.7/1.2	1.8/2.0	0.0/–0.1
37	2008-03-10	4 d	1.9/2.2	0.8/1.1	1.8/1.8	–0.2/–0.3
38	2010-11-09	5 d	1.7/2.2	0.6/1.2	1.6/1.7	–0.2/–0.2
39	2011-02-02	4 d	1.7/1.8	0.4/0.5	1.7/1.8	–0.3/–0.6

3.2 General results

In general we saw the largest improvement by the nudging results for the variable p.m.s.l. For every time series of the nudging runs at nearly all verified stations the RMSE and biases of p.m.s.l. were better than those of the normal forecast runs. There were only a few exceptions at storm events before 1980. For wind speed and direction the forecast without nudging was better for a few stations compared to the nudging runs, but not averaged over all stations.

Comparing all storms (except number one from 1962, where we have no observation data) we see that the RMSE of both COSMO-eu and COSMO-de for v_{10m} is between 1.6 m s^{-1} and 3.9 m s^{-1} , while the higher values mainly occur at older events (before and in 1983, see Table 1). This is also the case for the variable p.m.s.l. For dd_{10m} no tendency could be observed. If we compare COSMO-eu and COSMO-de we have no significant difference for the RMSE of v_{10m} of COSMO-eu and COSMO-de averaged over all storms. The same is valid for p.m.s.l. and dd_{10m} . The results of the RMSE of v_{10m} for the nudging runs are better or equal compared to the forecast runs for nearly all storms, except for the storms 2, 7, 8 and 9 for COSMO-eu and 2, 5, 8, 9, 13, 15, 19 and 23 for COSMO-de (see Table 1). For dd_{10m} we qualitatively get the same result, but for p.m.s.l. all nudging runs yield better or equal results as the normal forecast runs.

One reason for the improved results of newer events can be the better quality and higher resolution of the ERAInterim data for storms from 1979 on. Another reason for the improved results of the nudging runs is surely the rapid increase of observation data during the time of the occurrence of the storm events.

Comparing the biases of p.m.s.l. we obtain nearly the same values for COSMO-eu and COSMO-de. We have a small positive bias for normal forecast runs and values around zero for the nudging runs. The standard deviations of the biases are in the range as the biases themselves as we have seen for storm “Tilo”. For dd_{10m} COSMO-eu has a slightly positive bias, which is lower for the nudging runs compared to the forecast runs. COSMO-de has a minimally lower bias than COSMO-eu, averaged over all storms. The standard deviation of the biases of dd_{10m} is in the range of the biases themselves or even a little bit larger due to the different characteristics of the observation points. The wind speed biases of COSMO-eu and COSMO-de have a similar magnitude, but different sign, positive for COSMO-eu and negative for COSMO-de. Averaged over all storms the positive biases for COSMO-eu are $0.4 \pm 1.4 \text{ m s}^{-1}$ for runs with nudging and $0.7 \pm 1.5 \text{ m s}^{-1}$ without nudging. The negative biases for COSMO-de are $-0.3 \pm 1.6 \text{ m s}^{-1}$ for runs with nudging and $-0.4 \pm 1.6 \text{ m s}^{-1}$ without nudging.

Where does this big difference of wind speed bias (0.7 m s^{-1} for nudging runs respectively 1.1 m s^{-1} without nudging) of both COSMO models comes from? There could be two reasons where the differences result from. One answer is the different mesh width, which will influence the wind speed at grid points near the coast. However, looking at a map of the mean wind speed difference of COSMO-eu and COSMO-de (see Fig. 5) we see the main difference over land outside the Alps which is the result of different roughness length, z_0 . The differences in z_0 comes from the usage of different land use classifications. For COSMO-eu z_0 was derived from the GLC2000 data set (Bartholomé and Belward, 2005), whereas for COSMO-de the newer GlobCover

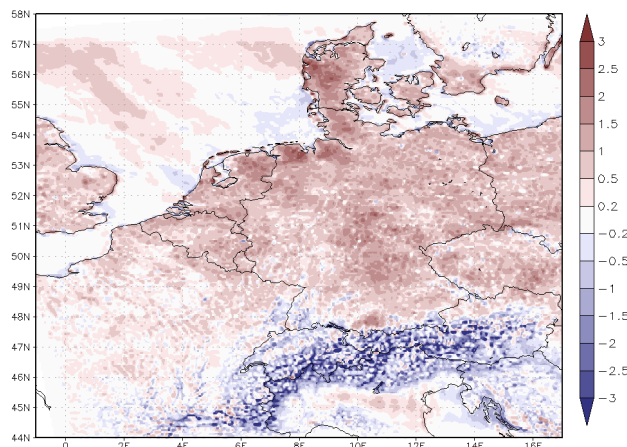


Figure 5. Difference of v_{10m} for COSMO-eu minus COSMO-de (nudging runs), averaged about the storm event (96 h) of “Tilo” 2007.

data set (Arino et al., 2008) has been employed. Outside the Alps z_0 is higher in the data derived from GlobCover which yields lower near surface winds, which are in better accordance with the observations. In the Alps z_0 for COSMO-eu contains an additional contribution from the orographic variability. We ran COSMO-eu with z_0 derived from GlobCover for three storms (“Tilo” 2007, “Kyrill” 2007, and “Britta” 2006). The wind speed bias of COSMO-eu decreased by 0.2 m s^{-1} averaged over all stations, 0.1 m s^{-1} for sea stations and 0.35 m s^{-1} for land stations which is an improvement for the storm. We conclude GlobCover yields better roughness values for COSMO-eu than GLC2000.

4 Summary

To improve the storm flood model of the NLWKN, DWD produced high-resolution spatial and temporal wind fields of 39 historical storms in the North Sea. The data are available for COSMO-eu and COSMO-de, both, in forecast and in nudging mode. I.e. we have a mini ensemble with 4 members for each storm event.

As expected we got better results for the nudging runs than for the normal forecasts for the RMSE as well as for the biases, with exception of the COSMO-de wind biases, where no clear tendency can be seen. Comparing COSMO-eu and COSMO-de we see no significant difference in the RMSE. The biases of COSMO-eu and COSMO-de differ significantly for the 10 m wind where COSMO-eu overestimates both values. The biases of COSMO-eu and COSMO-de for p.m.s.l. differ only marginally and are both very low.

Looking for the reason of the significant difference of the 10 m wind between COSMO-eu and COSMO-de, we detected big difference in the roughness length z_0 because it was derived from different land use data sets. The wind speed bias of COSMO-eu over land could be reduced by 0.35 m s^{-1} if z_0

was derived from GlobCover as has been done for COSMOde. A second reason could be the different mesh width of both models.

Further experiments will be made changing tuning parameters in the turbulence scheme of the COSMO model, and with wind speed dependent Charnock constant to calculate the sea surface roughness.

Edited by: M. M. Miglietta

Reviewed by: two anonymous referees

References

- Arino, O., Bicheron, P., Achard, F., Latham, J., Witt, R., and Weber, J.-L.: GlobCover the most detailed portrait of Earth, *ESA Bulletin*, 136, 25–31, 2008.
- Baldauf, M., Seifert, A., Förstner, J., Majewski, D., Raschendorfer, M., and Reinhardt, T.: Operational Convective-Scale Numerical Weather Prediction with the COSMO model: Description and Sensitivities, *Mon. Weather Rev.*, 139, 3887–3905, 2011.
- Bartholomé, E. and Belward, A. S.: GLC2000: a new approach to global land cover mapping from Earth observation data, *Int. J. Remote Sens.*, 26, 1959–1977, 2005.
- Bundesamt für Seeschifffahrt und Hydrographie (BSH), Storm flood classification: <http://www.bsh.de>, last access: 7 January 2014.
- Consortium for Small-scale Modelling, COSMO documentation: <http://www.cosmo-model.org>, last access: 7 January 2014.
- Dee, D. P., Uppala, S. M., Simmons, A. J., Berrisford, P., Poli, P., Kobayashi, S., Andrae, U., Balmaseda, M. A., Balsamo, G., Bauer, P., Bechtold, P., Beljaars, A. C. M., van de Berg, L., Bidlot, J., Bormann, N., Delsol, C., Dragani, R., Fuentes, M., Geer, A. J., Haimberger, L., Healy, S. B., Hersbach, H., Hólm, E. V., Isaksen, L., Kållberg, P., Köhler, M., Matricardi, M., McNally, A. P., Monge-Sanz, B. M., Morcrette, J.-J., Park, B.-K., Peubey, C., de Rosnay, P., Tavolato, C., Thépaut, J.-N., and Vitart, F.: The ERA-Interim reanalysis: configuration and performance of the data assimilation system, *Q. J. Roy. Meteorol. Soc.*, 137, 553–597, 2011.
- Frank, H. and Majewski, D.: Hindcasts of historic storms with the DWD models GME, LMQ and LMK using ERA-40 reanalyses, 2006, *ECMWF Newsletter*, 109, 16–21, 2006.
- Jensen, J., Mudersbach, C., Müller-Navarra, S. H., Bork, I., Koziar, C., and Renner, V.: Modellgestützte Untersuchungen zu Sturmfluten mit sehr geringen Eintrittswahrscheinlichkeiten an der deutschen Nordseeküste, *Die Küste*, 71, 123–167, 2006.
- Majewski, D., Liermann, D., Prohl, D., Ritter, B., Buchhold, B., Hanisch, T., Paul, G., Wergen, W., and Baumgardner, J.: The Operational Global Icosahedral-Hexagonal Gridpoint Model GME: Description and High-Resolution Tests, *Mon. Weather Rev.*, 130, 319–338, 2002.
- Schraff, C. H.: Mesoscale Data Assimilation and Prediction of Low Stratus in the Alpine Region, *Meteorol. Atmos. Phys.*, 64, 21–50, 1997.
- Schraff, C. and Hess, R.: Datenassimilation für das LM. promet, *Jahrgang 27*, Nr. 3/4, 156–164, 2002.
- Stauffer, D. R. and Seaman, N. L.: Use of Four-Dimensional Data Assimilation in a Limited-Area Mesoscale Model Part I: Experiments with synoptic scale data, *Mon. Weather Rev.*, 118, 1250–1277, 1990.
- Stauffer, D. R. and Seaman, N. L.: Multiscale four-dimensional data assimilation, *J. Appl. Meteorol.*, 33, 416–434, 1994.
- Uppala, S. M., Kållberg, P., Simmons, A., Andrae, U., da Costa Bechtold, V., Fiorino, M., Gibson, J., Haseler, J., Hernandez, A., Kelly, G., Li, X., Onogi, K., Saarinen, S., Sokka, N., Allan, R., Andersson, E., Arpe, K., Balmaseda, M., Beljaars, A., van de Berg, L., Bidlot, J., Bormann, N., Caires, S., Chevallier, F., Dethof, A., Dragosavac, M., Fisher, M., Fuentes, M., Hagemann, S., Hólm, E., Hoskins, B., Isaksen, L., Janssen, P., Jenne, R., McNally, A., Mahfouf, J.-F., Morcrette, J.-J., Rayner, N., Saunders, R., Simon, P., Sterl, A., Trenberth, K., Untch, A., Vasiljevic, D., Viterbo, P., and Woollen, J.: The ERA-40 re-analysis, *Q. J. Roy. Meteorol. Soc.*, 131, 2961–3012, 2005.
- Wiegand, P.: Küstenfibel – Ein Abc der Nordseeküste, Westholsteinische Verlagsgesellschaft Boyens & Co., Heide in Holstein, 1990.